

## MAGNETIC FIELDS IN COSMOLOGICAL SIMULATIONS OF DISK GALAXIES

RÜDIGER PAKMOR<sup>1</sup>, FEDERICO MARINACCI<sup>1,2</sup> AND VOLKER SPRINGEL<sup>1,2</sup>

*Draft version September 24, 2018*

### ABSTRACT

Observationally, magnetic fields reach equipartition with thermal energy and cosmic rays in the interstellar medium of disk galaxies such as the Milky Way. However, thus far cosmological simulations of the formation and evolution of galaxies have usually neglected magnetic fields. We employ the moving-mesh code AREPO to follow for the first time the formation and evolution of a Milky Way-like disk galaxy in its full cosmological context while taking into account magnetic fields. We find that a prescribed tiny magnetic seed field grows exponentially by a small-scale dynamo until it saturates around  $z = 4$  with a magnetic energy of about 10% of the kinetic energy in the center of the galaxy’s main progenitor halo. By  $z = 2$ , a well-defined gaseous disk forms in which the magnetic field is further amplified by differential rotation, until it saturates at an average field strength of  $\sim 6\mu\text{G}$  in the disk plane. In this phase, the magnetic field is transformed from a chaotic small-scale field to an ordered large-scale field coherent on scales comparable to the disk radius. The final magnetic field strength, its radial profile and the stellar structure of the disk compare well with observational data. A minor merger temporarily increases the magnetic field strength by about a factor of two, before it quickly decays back to its saturation value. Our results are highly insensitive to the initial seed field strength and suggest that the large-scale magnetic field in spiral galaxies can be explained as a result of the cosmic structure formation process.

*Subject headings:* methods: numerical — magnetohydrodynamics — galaxies: formation — galaxies: evolution

### 1. INTRODUCTION

Numerous observations have shown that the Universe is highly magnetized on a variety of scales, ranging from stars to galaxies, and even up to clusters of galaxies. Among these objects, galaxies are special because their magnetic energy content appears to be roughly in equipartition with the thermal energy of the gas and the energy stored in cosmic rays (Beck et al. 1996). Consequently, magnetic fields are potentially quite relevant for the dynamical evolution of galaxies, as well as for the regulation of their star formation rate (Beck 2009).

The origin and evolution of galactic magnetic fields is still not well understood. Tiny initial magnetic seed fields are assumed to be generated either in the primordial Universe or by Biermann batteries in the first stars (Kulsrud & Zweibel 2008). Different processes have been proposed for subsequently amplifying the magnetic field to the observed present-day strength, including turbulent dynamo processes (see, e.g. Kulsrud et al. 1997; Arshakian et al. 2009; Schleicher et al. 2013), shear flows during structure formation (see, e.g. Dolag et al. 1999), or a Galactic dynamo (Hanasz et al. 2004, for a review see Widrow 2002). A number of these scenarios have been studied with numerical magnetohydrodynamics simulations, either concentrating on isolated disk galaxies (Hanasz et al. 2009; Kotarba et al. 2009; Wang & Abel 2009; Dubois & Teyssier 2010; Pakmor & Springel 2013) or on larger scales in a cosmological context, ranging from galactic halos (Beck et al. 2012, 2013a) to galaxy clusters (Dolag et al. 1999; Dubois & Teyssier 2008; Donnert et al. 2009) and voids (Beck et al. 2013b).

However, until quite recently, the problem of successfully

forming disk galaxies from cosmological initial conditions with properties similar to observed spiral galaxies has essentially been unsolved, precluding the possibility of direct cosmological predictions of the expected magnetic field topology and strength in disk galaxies. Here, we present the first high-resolution hydrodynamical simulation of the formation of a Milky-Way like galaxy in its full cosmological context including magnetic fields. We make use of the same simulation approach as in Marinacci et al. (2014) but add magnetic fields that are fully coupled to the hydrodynamical evolution. This allows us to produce realistic disc galaxies while at the same time obtaining predictions for the magnetic field strength throughout the galaxy as well as its impact on the global star formation efficiency. In §2 we briefly summarize our numerical methodology and specify our initial conditions. Results for the amplification of the magnetic field in the modelled galaxy are discussed in §3, while the present-day structure of the field in the formed disc galaxy is analyzed in §4. We draw our conclusions in §5.

### 2. SETUP

We simulate the formation of a Milky-Way sized galaxy in a cosmological volume using the “zoom-in technique”. To this end we adopt the initial conditions of halo Aq-A-4 from the ‘Aquarius’ project (Springel et al. 2008). The halo was selected from the ‘Millennium II’ simulation (Boylan-Kolchin et al. 2009) with a mass similar to the Milky Way and applying a mild isolation criterion to ensure a relatively quiet merger history, which favors the formation of an extended disk. Indeed, the halo evolves quietly for most of the time, with the exception of a minor merger around  $z = 1$ . Our simulation features a baryonic mass resolution of  $5 \times 10^4 M_{\odot}$ , a dark matter mass resolution of  $3.2 \times 10^5 M_{\odot}$  and a gravitational softening of 340 pc. At this resolution, our simulation is comparable to some of the best resolved cosmological galaxy formation simulations available today.

<sup>1</sup> Heidelberger Institut für Theoretische Studien, Schloss-Wolfsbrunnengasse 35, 69118 Heidelberg, Germany

<sup>2</sup> Zentrum für Astronomie der Universität Heidelberg, Astronomisches Recheninstitut, Mönchhofstr. 12-14, 69120 Heidelberg, Germany

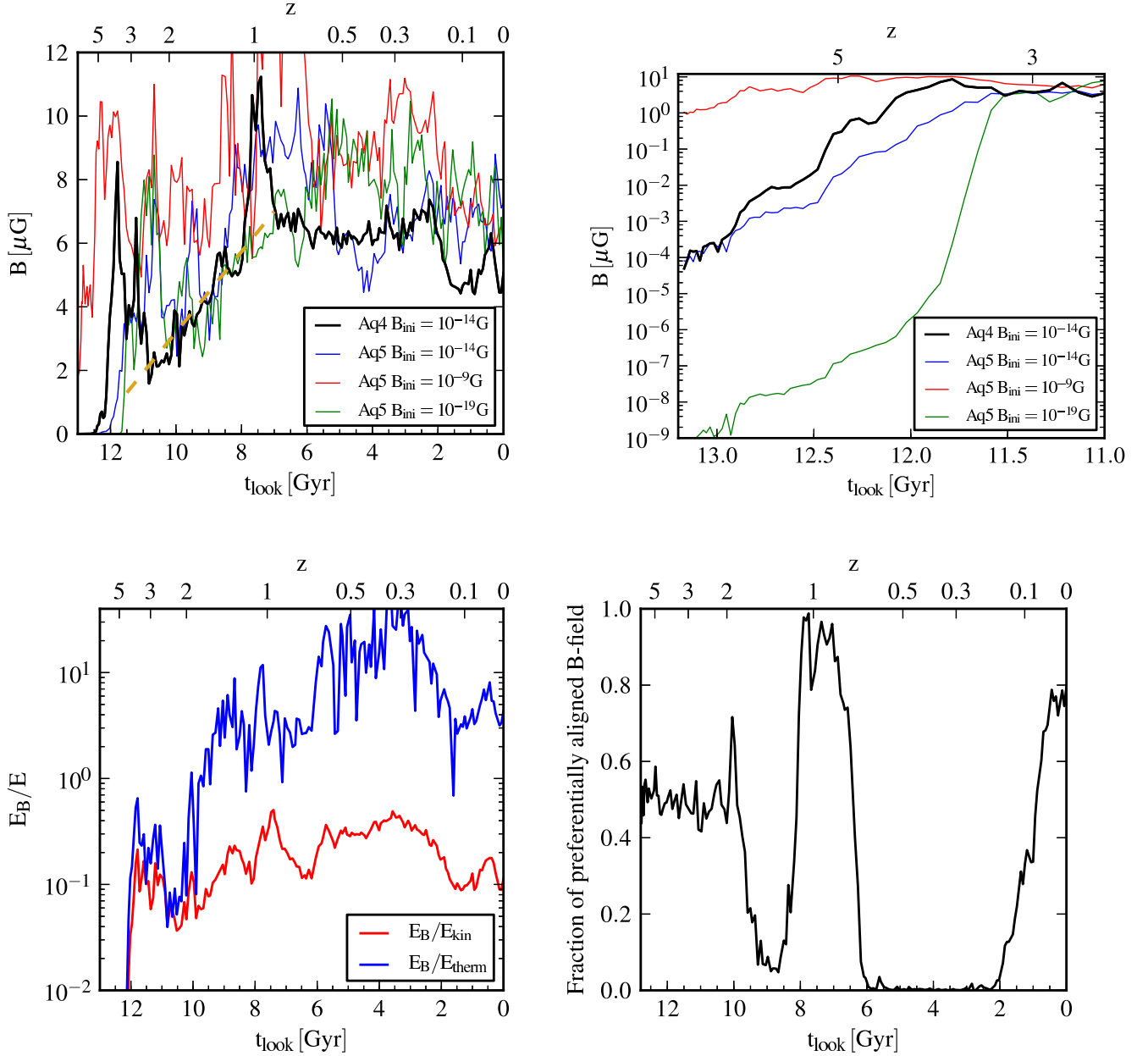


**Figure 1.** Evolution of the volume weighted average root mean square magnetic field strength (top panels), the ratio of magnetic energy to kinetic energy and thermal energy (bottom left panel), and the volume fraction in which the magnetic field is preferentially aligned with the velocity field (bottom right panel) in a disk with physical radius 15 kpc and height 2 kpc centered on the potential minimum of the halo and orientated along the principal axes of all stars within 10% of the virial radius. The bulk velocity of the galaxy has been removed before calculating the kinetic energy. Although there is no prominent disk at  $z > 2$ , we use the same volume cut to make the comparison easier. The top panels show additional runs with 8 times lower mass resolution (Aq-A-5) and different magnetic seed field strength. The yellow line in the top left panel indicates the approximately linear growth of the magnetic field strength between  $z = 2$  and  $z = 1$ .

We employ the moving-mesh code AREPO (Springel 2010) and its new ideal MHD implementation (Pakmor et al. 2011; Pakmor & Springel 2013). AREPO combines advantages of Lagrangian codes (e.g. small advection errors and automatic adaptivity) with advantages of Eulerian codes (e.g. accurate gradient estimates, fast convergence rate, and no need for an artificial viscosity), making it a particularly well-matched technique for the problem at hand. Our model for baryonic physics (see Vogelsberger et al. 2013, for a full description) includes primordial and metal line cooling, a sub-grid model for the interstellar medium (ISM) and star for-

mation (Springel & Hernquist 2003), a self-consistent treatment of stellar evolution and chemical enrichment, as well as galactic-scale winds (implemented with a kinetic scheme similar to Puchwein & Springel 2013) and supermassive black hole growth and feedback. The code’s configuration and the setup of the employed baryonic physics modules is identical to the suite of simulations presented in Marinacci et al. (2014), to which we refer for further details, except for the addition of magnetic fields.

We introduce the magnetic field in the initial conditions of

the simulation in terms of a homogeneous comoving<sup>3</sup> seed field with a strength of  $10^{-14}$  G, and follow its evolution in the ideal MHD approximation. At the initial redshift  $z = 127$  this is equivalent to a physical magnetic field strength of  $2 \times 10^{-5} \mu\text{G}$ . We note that when stars form from a gas cell as part of the subgrid model, we assume that the corresponding magnetic field flux is locked up into the star and removed with the gas. Compared to not removing the magnetic field (as done in Pakmor & Springel 2013) this assumption leads to slightly smaller (by at most a few tens of percent) magnetic field strength. Also note that this can introduce a small divergence error into the local magnetic field, however, our MHD implementation is robust enough to quickly eliminate any such local error.

### 3. AMPLIFICATION OF THE MAGNETIC FIELD

The time evolution of the average magnetic field strength in the disk is shown in Fig. 1 (top left panel). The field strength grows exponentially until it reaches a few  $\mu\text{G}$  around  $z = 4$ . At this time, the magnetic energy attains about 10% of the kinetic, and 20% of the thermal energy. Such a large magnetic field already at high redshift is consistent with recent observations (Kronberg et al. 2008). Even though strong fluctuations occur, we note there is no significant further net amplification of the magnetic field and no evident large-scale ordering before the galaxy forms a well-defined disk at about  $z = 2$ .

This early evolution of the magnetic field is consistent with a turbulent small-scale dynamo seen in previous simulations of magnetic field growth in cosmological halos (Dolag et al. 1999; Beck et al. 2012) and predicted analytically (Schober et al. 2013). However, in contrast to the analytical models the main driver of turbulence in the ISM of our simulation are accretion flows onto the forming galaxy. We do not take supernovae into account as a source of turbulence, because our sub-scale model for star formation and supernova feedback does not treat them explicitly (Springel & Hernquist 2003). It is thus particularly interesting that our primordial magnetic seed field is amplified to saturation already at high redshifts through structure growth processes alone, indicating that supernova feedback may not be necessary to amplify fields to  $\mu\text{G}$  strength in young galaxies. This may be important in particular for the magnetic field amplification in dwarf galaxies. We stress that the strength at which the magnetic field saturates in this early evolution does not depend on the size or orientation of the initial seed field. As Fig. 1 (top right panel) shows, saturation is always reached before  $z = 3$  and the saturation strength depends only very weakly on the initial seed field because of the fast exponential amplification, in agreement with the findings in Beck et al. (2012). Only a too large initial magnetic field will cause a problem, since it can lead to a larger saturation strength.

After the disk has formed around  $z = 2$ , the magnetic field strength grows approximately linearly with time, until it again saturates, at an average field strength of about  $6 \mu\text{G}$ . This linear growth due to differential rotation in the disk is the same as found in simulations of isolated disk galaxies (Hanasz et al. 2009; Dubois & Teyssier 2010; Pakmor & Springel 2013). For a simulation with identical initial conditions but eight times lower mass resolution (run Aq-A-5 in the Aquarius naming convention), we find that the final field strength is essentially the same, suggesting that this quantity is quite well converged (Fig. 1 top right panel). However, the magnetic

field strength fluctuates significantly more in the lower resolution runs.

Shortly after  $z = 2$ , the magnetic energy has reached equipartition with the thermal energy as a result of an increase of the magnetic energy as well as a decrease of the thermal energy. It also reaches about 20% of the kinetic energy at  $z = 1$ . For the following 8 Gyrs,  $E_B/E_{\text{kin}}$  and  $E_B/E_{\text{thermal}}$  fluctuate between 0.2 to 0.5 and 3 to 20, respectively (see Fig. 1 bottom left panel).

The differential rotation in the gas disk also orders the magnetic field on the scale of the disk. Once the disk has formed, the magnetic field is transformed on a timescale of about 2 Gyrs from a randomly oriented small-scale field to a configuration in which it is ordered on scales comparable to the disk, with an alignment along the azimuthal velocity field. Since the ideal MHD equations are symmetric under a global sign flip of the  $B$ -field, we do not expect that either the parallel or anti-parallel orientation relative to the velocity field is preferred. Nevertheless, one of these directions typically ends up prevailing over the other, with most of the disk showing either the parallel or anti-parallel orientation. Moreover, the dominant orientation is not necessarily permanent, but can reverse on a typical timescale of about 2 Gyrs if the disk is sufficiently perturbed. We show this in Fig. 1 (bottom right panel), where we plot the fraction of the magnetic field aligned with the gas velocity field. There is no dominant alignment until about  $z = 2$ , but then the field becomes almost completely anti-aligned with the velocity field at  $z \sim 1.5$ , followed by a reversal of the orientation and an eventual switch back to the anti-aligned orientation on a timescale of about 2 Gyrs between each reversal. After this phase, the  $B$ -field stays completely anti-aligned for more than 4 Gyrs, but starts changing again in the last 2 Gyrs to reach a predominantly aligned orientation at  $z = 0$ .

We note that the average magnetic field strength peaks close to  $z = 1$  when a minor merger occurs (see Marinacci et al. 2014). In this merger, the mean field strength is amplified by almost a factor of two, but then decays back to its prior saturation value in about one Gyr. An amplification during mergers has also been observed in dedicated simulations of isolated galaxy mergers (Kotarba et al. 2011; Geng et al. 2012).

### 4. THE GALAXY AT $Z=0$

The projected stellar density as well as slices through the gas density and velocity fields in the disk plane at  $z = 0$  are shown in Fig. 2. Similarly to the non-MHD runs discussed in detail in Marinacci et al. (2014), a rotationally supported disk galaxy with realistic stellar mass and scale length has formed. The gas shows a very regular circular velocity field in the disk plane, and spiral structures are visible in the density and velocity fields. The vertical velocity and density structures are dominated by irregular bipolar outflows as a result of our kinetic wind implementation, which launches winds preferentially along the galaxy's spin axis.

Fig. 3 presents the magnetic field configuration of our galaxy at  $z = 0$ . The azimuthal magnetic field in the disk is mostly oriented parallel to the velocity field (see also Fig. 1 bottom right panel). Its sign relative to the direction of the velocity field changes in magnetic spiral arms that correlate with the spiral structure of the density field. The orientation of the magnetic field perpendicular to the disk exhibits no clear correlation with the velocity field and changes on scales of order the vertical disk scale height.

The magnetic field strength reaches about  $15 \mu\text{G}$  close to

<sup>3</sup>  $B_{\text{comoving}} = a^2 B_{\text{physical}}$ , where  $a$  is the scale factor.

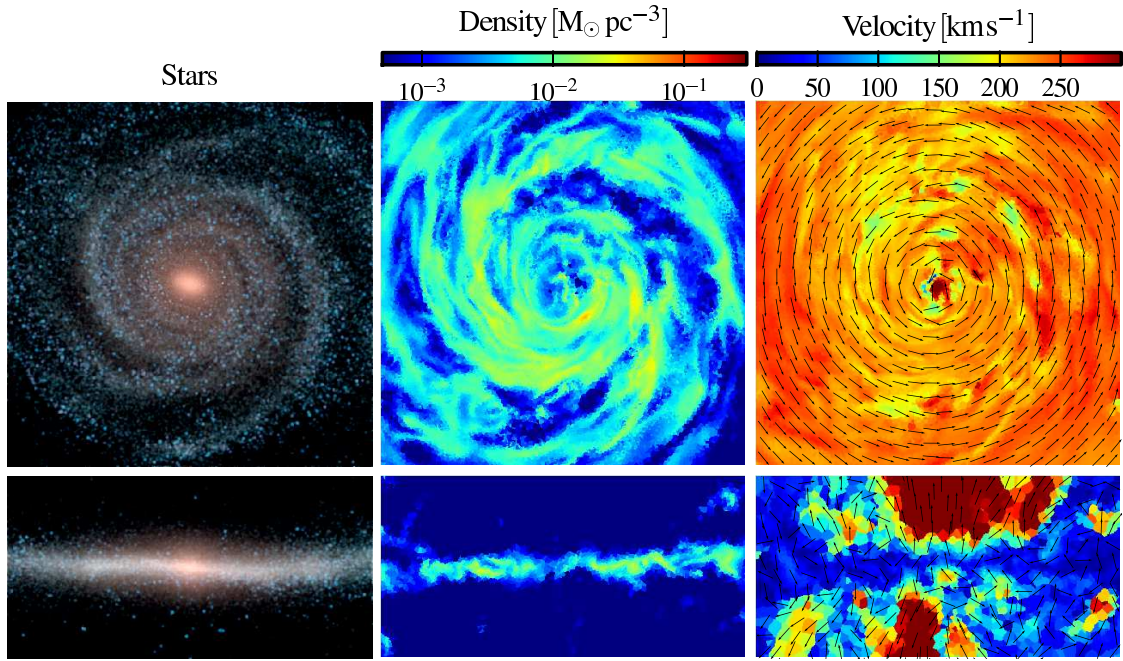


**Figure 2.** The stellar and gaseous disk at redshift  $z = 0$ . The column on the left shows the projected stellar density using a logarithmic mapping of  $K$ -,  $B$ - and  $U$ -band luminosity of the stars to a RGB-composite. The middle and right columns display, respectively, slices through the center of the galaxy of the gas density and the horizontal (top panel) and vertical (bottom panel) velocity fields. The coordinate system shown has been oriented along the principal axes of all stars within 10% of the virial radius, and the bulk velocity of the galaxy has been removed. Top and bottom rows give face-on and edge-on views, respectively. The panels on the right include overlaid arrows to indicate the velocity vector field. The region shown is a box with a width of 50 kpc.

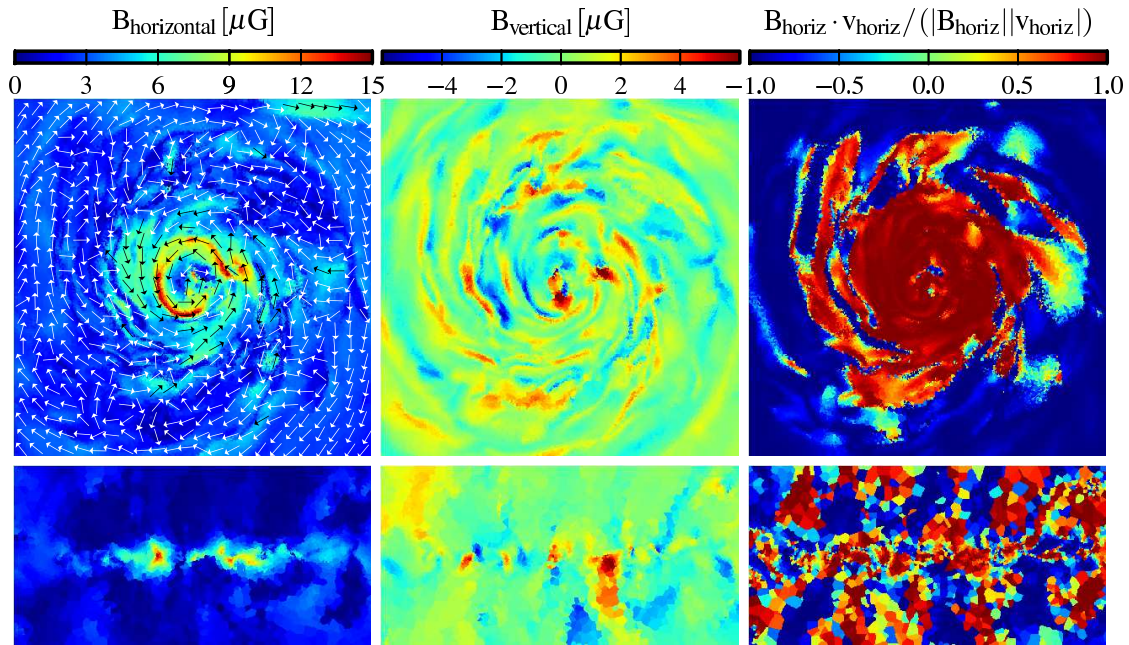


**Figure 3.** The magnetic field in the disk at redshift  $z = 0$ . Similar to Fig. 2, but now showing slices of the magnetic field strength in the disk plane (left column), the component of the magnetic field perpendicular to the disk plane (middle column), and the orientation of the magnetic field relative to the orientation of the velocity field (right column). In the top left panel, black and white arrows have been overlaid to indicate the direction of the magnetic field in the disk.

the center of the disk and a few  $\mu\text{G}$  in the outer parts, in good agreement with the magnetic field inferred for observed spiral galaxies (see, e.g. Beck et al. 1996; Beck 2009; Basu & Roy 2013). The magnetic field component perpendicular to the disk is significantly smaller compared with the azimuthal component and also changes sign in spiral arms. The magnetic field strength in the very center of the disk is comparable to values at larger radii of the order of one kpc, because

the central supermassive black hole included in our simulations blows out dense, highly magnetized gas from the galactic centre, lowering the gas density and magnetization there. This may potentially cause an underestimate of the innermost field strength if this outflow is overly strong.

The radial and vertical profiles of the magnetic field strength for different redshifts between  $z = 2$ , when the disk first forms, and  $z = 0$  are shown in Fig. 4. At  $z = 2$ , the field

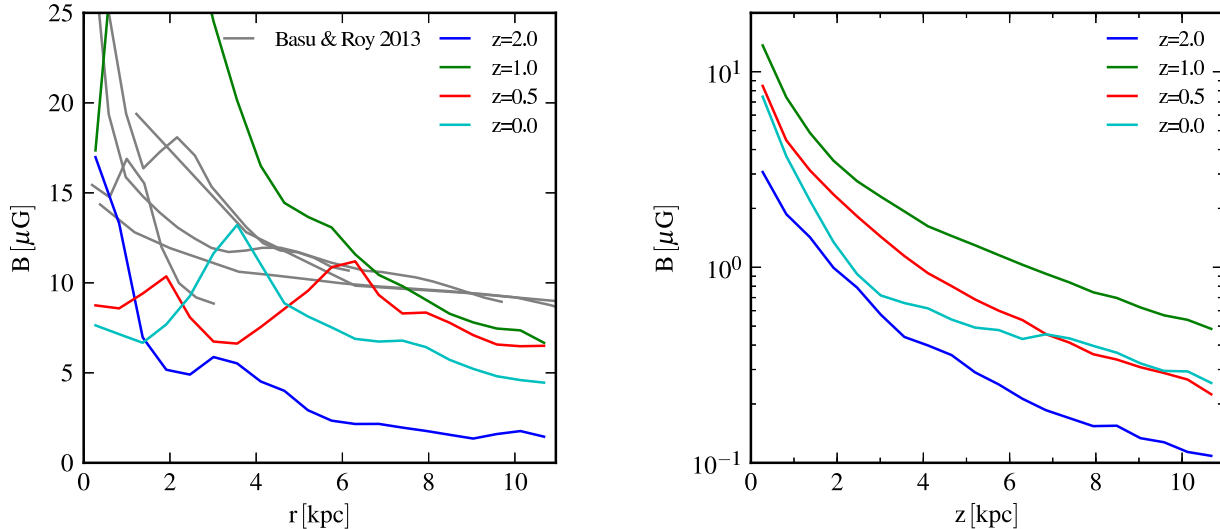


**Figure 4.** Magnetic field strength profiles in the radial (left panel) and  $z$  directions (right panel). The panels show the volume-weighted average root mean square  $B$ -field strength, using radial bins with a total height of 1 kpc centered on the disk plane for the radial profile, and using height bins at a constant radius of 15 kpc for the vertical profile averaged over both sides of the disk. The grey lines in the left panel show the field strength profiles inferred by Basu & Roy (2013) for five observed galaxies.

reaches about  $15 \mu\text{G}$  close to the center of the disk and then declines roughly linearly with radius to a value of only  $1 \mu\text{G}$  at radii larger than a few kpc. At  $z = 1$ , the radial magnetic field has grown at all radii. It reaches  $30 \mu\text{G}$  close to the center, and  $7 \mu\text{G}$  to  $15 \mu\text{G}$  at radii between 5 kpc and 10 kpc due to a minor merger at that redshift. At  $z = 0.5$ , the magnetic field has dropped again at radii smaller than 6 kpc, and most notably peaks now around a radius of 6 kpc with a field strength of only about  $10 \mu\text{G}$ , as the temporary amplification triggered by the minor merger fades away. From  $z = 0.5$  to  $z = 0$  the magnetic field hardly evolves. As shown in Fig. 4, the radial profile of the field strength at  $z = 0$  agrees well with profiles observed for some spiral galaxies (Basu & Roy 2013). In the vertical direction, the magnetic field strength declines exponentially, quickly dropping below  $1 \mu\text{G}$  at heights larger than a few kpc. The overall time evolution of the vertical profile follows closely that found for the radial profile.

## 5. CONCLUSION

The hydrodynamical cosmological simulation presented here is the first successful formation of a present-day Milky Way-like disk galaxy in which the dynamics of magnetic fields has been included. Starting with a tiny seed field, we find that the field is amplified first by an exponential small-scale dynamo, and later by differential rotation in the disk after it formed. The field strength grows roughly to equipartition in the ISM but has only a minor effect on the global star formation history of the galaxy, at least at late times. Compared with the corresponding non-MHD simulations of Marinacci et al. (2014), we find an equally well defined disk morphology, and almost the same stellar mass.

Interestingly, the strength and shape of the magnetic field predicted by our simulations agrees rather well with observational data. Given the lack of any free parameters in our modelling of the magnetic field (recall that the results are invariant with respect to the seed field strength over a very wide range), this is a non-trivial outcome that shows that large-scale galactic fields can in principle be well understood as a result of structure growth alone. We also note that our results are nu-

merically robust and converged, although we concede that the unresolved small-scale dynamics in the ISM remains a source of uncertainty.

The full three-dimensional magnetic field structure we predict in our simulation can in principle be used to refine models for the propagation of charged particles in galaxies such as the Milky Way. In fact, it is a tantalizing prospect to compute yet much higher resolution models in the future, and then to carry out detailed comparisons between the simulated magnetic field properties both with observations and models of the magnetic field of the Milky Way (Jansson & Farrar 2012a,b; Oppermann et al. 2012). This will allow us to significantly improve our understanding of the evolution of galactic magnetic fields in the Universe. Moreover, the ability to simulate magnetic fields in galaxy formation allows the addition of cosmic rays and of a proper treatment of their transport along the field lines. Such a consistent treatment will be needed to accurately study the mechanism and relevance of cosmic ray driven winds (see, e.g. Ptuskin et al. 1997; Uhlir et al. 2012; Hanasz et al. 2013), which have been conjectured to be a highly important feedback mechanism especially in small galaxies.

## ACKNOWLEDGEMENTS

We thank the referee for a constructive and critical report. F.M. acknowledges support by the DFG Research Centre SFB-881 ‘The Milky Way System’ through project A1. R.P. acknowledges support by the European Research Council under ERC-StG grant EXAGAL-308037. V.S. thanks for support by Priority Programme 1648 ‘SPPEXA’ of the German Science Foundation, and by the Klaus Tschira Foundation. Simulations of this paper used the SuperMUC computer at the Leibniz Computing Centre, Garching, under project PR85JE of the Gauss Centre for Supercomputing, Germany.

## REFERENCES

- Arshakian, T. G., Beck, R., Krause, M., & Sokoloff, D. 2009, *A&A*, 494, 21  
 Basu, A., & Roy, S. 2013, *MNRAS*, 433, 1675

- Beck, A. M., Dolag, K., Lesch, H., & Kronberg, P. P. 2013a, MNRAS, 435, 3575
- Beck, A. M., Hanasz, M., Lesch, H., Remus, R.-S., & Stasyszyn, F. A. 2013b, MNRAS, 429, L60
- Beck, A. M., Lesch, H., Dolag, K., et al. 2012, MNRAS, 422, 2152
- Beck, R. 2009, *Astrophysics and Space Sciences Transactions*, 5, 43
- Beck, R., Brandenburg, A., Moss, D., Shukurov, A., & Sokoloff, D. 1996, ARA&A, 34, 155
- Boylan-Kolchin, M., Springel, V., White, S. D. M., Jenkins, A., & Lemson, G. 2009, MNRAS, 398, 1150
- Dolag, K., Bartelmann, M., & Lesch, H. 1999, A&A, 348, 351
- Donnert, J., Dolag, K., Lesch, H., & Müller, E. 2009, MNRAS, 392, 1008
- Dubois, Y., & Teyssier, R. 2008, A&A, 482, L13
- 2010, A&A, 523, A72
- Geng, A., Kotarba, H., Bürzle, F., et al. 2012, MNRAS, 419, 3571
- Hanasz, M., Kowal, G., Otmianowska-Mazur, K., & Lesch, H. 2004, ApJ, 605, L33
- Hanasz, M., Lesch, H., Naab, T., et al. 2013, ApJ, 777, L38
- Hanasz, M., Wóltański, D., & Kowalik, K. 2009, ApJ, 706, L155
- Jansson, R., & Farrar, G. R. 2012a, ApJ, 757, 14
- 2012b, ApJ, 761, L11
- Kotarba, H., Lesch, H., Dolag, K., et al. 2011, MNRAS, 415, 3189
- 2009, MNRAS, 397, 733
- Kronberg, P. P., Bernet, M. L., Miniati, F., et al. 2008, ApJ, 676, 70
- Kulsrud, R., Cowley, S. C., Gruzinov, A. V., & Sudan, R. N. 1997, Phys. Rep., 283, 213
- Kulsrud, R. M., & Zweibel, E. G. 2008, *Reports on Progress in Physics*, 71, 046901
- Marinacci, F., Pakmor, R., & Springel, V. 2014, MNRAS, 437, 1750
- Oppermann, N., Junklewitz, H., Robbers, G., et al. 2012, A&A, 542, A93
- Pakmor, R., Bauer, A., & Springel, V. 2011, MNRAS, 418, 1392
- Pakmor, R., & Springel, V. 2013, MNRAS, 432, 176
- Ptuskin, V. S., Voelk, H. J., Zirakashvili, V. N., & Breitschwerdt, D. 1997, A&A, 321, 434
- Puchwein, E., & Springel, V. 2013, MNRAS, 428, 2966
- Schleicher, D. R. G., Latif, M., Schober, J., et al. 2013, *Astronomische Nachrichten*, 334, 531
- Schober, J., Schleicher, D. R. G., & Klessen, R. S. 2013, A&A, 560, A87
- Springel, V. 2010, MNRAS, 401, 791
- Springel, V., & Hernquist, L. 2003, MNRAS, 339, 289
- Springel, V., Wang, J., Vogelsberger, M., et al. 2008, MNRAS, 391, 1685
- Uhlig, M., Pfrommer, C., Sharma, M., et al. 2012, MNRAS, 423, 2374
- Vogelsberger, M., Genel, S., Sijacki, D., et al. 2013, MNRAS, 436, 3031
- Wang, P., & Abel, T. 2009, ApJ, 696, 96
- Widrow, L. M. 2002, *Reviews of Modern Physics*, 74, 775